ELSEVIER

Earth and Planetary Science Letters 120 (1993) 207–220

EPSL

A metamorphic history from micron-scale $^{207}Pb/^{206}Pb$ chronometry of Archean monazite

C.P. DeWolf [a], N. Belshaw [b], R.K. O'Nions [b]

[a] *Department of Geological Sciences, University of Michigan, Ann Arbor, MI 48109-1063, USA*
[b] *Department of Earth Sciences, University of Cambridge, Downing Site, Cambridge, CB1 3EQ, UK*

(Received May 28, 1993; revision accepted October 7, 1993)

Abstract

Ion microprobe measurements of Pb isotope ratios in monazites have been obtained, *in situ*, from thin sections using the Cambridge ISOLAB 120. Molecular interferences are sufficiently resolved at an RP of 6500 to allow $^{207}Pb/^{206}Pb$ dating of monazite with precisions as low as 4–5 Ma (2σ). The results presented here provide important information on the chronological history of the Late Archean metamorphism of the Wind River Range, Wyoming (USA).

Matrix monazites and monazite inclusions in garnets from a metapelite from the northern Wind River Range have been analysed by SIMS. In a previous study peak metamorphic conditions ($T = 800°C$; $P = 8 \pm 1$ kb *) were estimated using inclusion assemblages in garnets from this same sample. Isolated monazite inclusions in garnet yield $^{207}Pb/^{206}Pb$ age estimates of 2781 ± 6 to 2809 ± 10 Ma. Those along fractures yield lower ages (2603–2687 Ma) which are similar to TIMS and SIMS ages of matrix monazites. A single large (500 μm) monazite grain locally preserves growth zoning, but has a recrystallised core and a resorbed (recrystallised?) rim. Age estimates for these three regions are 2788 ± 9 Ma, 2663 ± 4 and 2523 ± 6 Ma, respectively. Thus the inclusion assemblages of Sharp and Essene * may record peak metamorphic conditions at ca. 2.8 Ga, and indicate a phase of metamorphism that predates by over 100 Ma the emplacement of the Bridger Batholith, the major lithologic component of the northern Wind River Range.

The analysed monazite grains appear to preserve ca. 300 Ma history, even within a single grain. Monazite inclusions in garnet that are fully armoured may provide estimates for the time of garnet growth, even in high grade terranes where most chronometers are reset. The age pattern preserved by the large monazite grain cannot be simply related to diffusion controlled closure. Instead, a chronology is preserved which can be related to the petrographic setting of individual grains through *in situ* analysis.

1. Introduction

It is now possible to develop quantitative models for the rates of heating, cooling, burial and uplift of metamorphic rocks during orogenesis. This development has been made possible by improved techniques for isotopic chronometry of metamorphic minerals applied in conjunction with thermobarometry of metamorphic assemblages. Several recent studies have used Sm–Nd [1,2], Rb–Sr [2,3] and U–Pb [2,5] isotope systematics of garnets to date their growth, thereby allowing

[UC]

* Sharp and Essene, 1991.

SSDI 0012-821X(93)E0187-0

calculation of burial, heating, uplift and cooling rates along metamorphic P–T paths. These studies have amply demonstrated that the key information may be preserved only on the sub-millimetre scale, but so far little use has been made of spatially resolved techniques of isotope analysis such as secondary ion mass spectrometry (SIMS) for minerals other than zircon.

Data obtained from SIMS analysis has been used extensively for *in situ* U–Pb geochronology of zircon [6–11]. However, its application to metamorphic studies has been restricted to the analysis of zircon overgrowths inferred to have grown during metamorphism [e.g., 12]. Unfortunately, the relationship between the timing of overgrowth formation and the formation of the metamorphic mineral assemblages, which may provide information on the physical conditions accompanying metamorphism, may be ambiguous. On the other hand, monazite, (Ce,La,Nd) PO_4, may be a more suitable phase for extracting *in situ* chronological information that relates to metamorphism. Monazite is a common accessory mineral in upper amphibolite and granulite facies rocks, particularly metapelites and leucocratic gneisses [12,13]. Several authors have suggested that monazite is unstable in rocks of pelitic composition below the amphibolite facies [12,14,15], though apparently detrital monazite has been identified in upper amphibolite paragneisses [14]. Although monazites typically have high Th and U contents (ca. 1–25 and 0.1–1.0 wt%, respectively), they frequently yield concordant ages in the U–Pb system without evidence for extensive Pb loss which is characteristic of zircons [14].

The frequent occurrence of monazite as inclusions in garnets of amphibolite facies metapelites is significant, because garnet is the most commonly used phase in the determination of P–T paths. Below ca. 600°C, diffusion rates are slow enough such that the Rb–Sr, U–Pb and Sm–Nd isotopic systems appear to preserve the time of garnet growth [5]. However, in upper amphibolite facies rocks, garnet U–Pb ages are typically older than Sm–Nd ages, possibly because Pb diffuses more slowly than Sm and Nd and the closure temperature for the Sm and Nd in garnet is exceeded [17]. Given the very low concentrations of U in garnet, U–Pb ages in garnet may be strongly influenced by inclusions of zircon [18] or monazite [19]. Zircon is unlikely to be useful in dating garnet growth because it is commonly an inherited mineral. Inheritance of radiogenic Pb appears to be less common in monazite but cannot be assumed to be absent *a priori*. If a link can be established between garnet and monazite growth, or if monazite U–Pb systematics remain "open" until incorporation in a growing garnet, U–Pb dating of monazite using SIMS at high spatial resolution may prove to be a useful method for dating garnet growth. In combination with careful thermobarometry, this approach may be particularly useful for deriving rates of heating, cooling, burial and uplift during orogenesis from the analysis of a few polished sections of metamorphic rock. Here, we present the results of our study of $^{207}Pb/^{206}Pb$ ages on monazites using high resolution SIMS on high-grade metapelites.

2. Geological setting

2.1. Previous work

The samples selected for this study are from the Archean core complex of the Wind River Range, Wyoming, USA. They are metapelites from the Crescent Lake region from where Sharp and Essene [1] estimated peak metamorphic conditions of 800 ± 50°C and 8 ± 1 kb. Previous geochronology in the Wind River Range has focused upon the late Archean granitoids for which whole-rock ages between 2670 and 2550 Ma have been reported [10,20]. The U–Pb ages of some zircons from the more deformed migmatites, obtained using both conventional and SIMS techniques [11] are significantly older and range from 3.2 and 3.8 Ga.

Ages have been obtained previously on bulk separates of minerals separated from the sample discussed in this study [19]. Abraded single and bulk fraction zircons yield an upper concordia intercept age ca. 2810 Ma, whereas garnets yield a $^{207}Pb/^{206}Pb$ age of 2751 ± 25 Ma. However, the bulk of the analysed U is contained in monazite inclusions within the garnet [19]. Separated mon-

azite fractions from the same sample yield a U–Pb age of 2659 ± 1 Ma (data presented in Table 1) and an eight-point garnet-matrix Sm–Nd isochron age of 2598 ± 17 Ma [19], suggesting metamorphism at ca. 2.8 Ga followed by closure of the various isotopic systems in these phases at lower temperature. No evidence has been found so far in these samples to support a metamorphic event as early as 3.2 Ga ago.

2.2. Sample descriptions

2.2.1. Samples SW-121 and DW-46

Samples SW-121 and DW-46 were collected within 1 m from the same outcrop of pelitic gneiss. They are petrographically indistinguishable and have an assemblage of biotite-cordierite-garnet-K-feldspar-plagioclase-quartz with inclusions of sillimanite in the garnet. Inclusion assemblages in SW 121 were used by Sharp and Essene [1] to infer peak metamorphic conditions of 800 ± 50 °C and 8 ± 1 Kb. Monazite occurs in this sample either as inclusions in garnet, or as part of the groundmass in association with quartz, plagioclase and biotite. Monazite inclusions in garnet are typically ≤ 50 μm across and are chemically variable with $0 < Th < 12$ wt%, $3 < Th/U < 45$ and $1.05 < La/Nd < 1.43$ [21]. Some of the inclusions are zoned showing a small increase (1 wt%) of Th and Th/U from core to rim [21]. Whereas the groundmass monazites associated with quartz or plagioclase display similar characteristics, ca. 20 μm monazite inclusions in biotite have significantly lower Th and U contents. Large (150–300 μm) monazites such as used for the TIMS U–Pb analyses [19] are irregularly zoned when viewed using back-scattered electron (BSE) imaging, with variations corresponding to 1–2 wt% Th.

2.2.2. Sample DW-9A

Sample DW-9A is from a 0.5 m garnet-biotite-rich layer within a felsic gneiss. The mineral assemblage is garnet-biotite-plagioclase-K-feldspar-quartz with sillimanite occurring as inclusions. Garnet shows some retrogression to biotite and plagioclase. Monazite occurs both as small inclusions within the garnet (< 50 μm) and as somewhat irregular large grains (100–500 μm) in the groundmass. Groundmass monazite grains show extreme zoning with Th reaching concentrations up to 25 wt% at the rims. The grains contain regions with lamellar zoning in Th content and irregular "patchy" zoning. The grain selected for SIMS analysis is typical of these (Fig. 1). It is approximately hexagonal in outline, clear yellow in plane-polarised light, and highly birefringent. Within the grain there are different regions with distinct chemical zonation patterns visible using back-scattered electron (BSE) imaging. These regions are site 6, a region with fine lamellar zoning parallel to a growth face, on a scale of 1–3 μm which is interpreted to be growth zoning; site 5, a

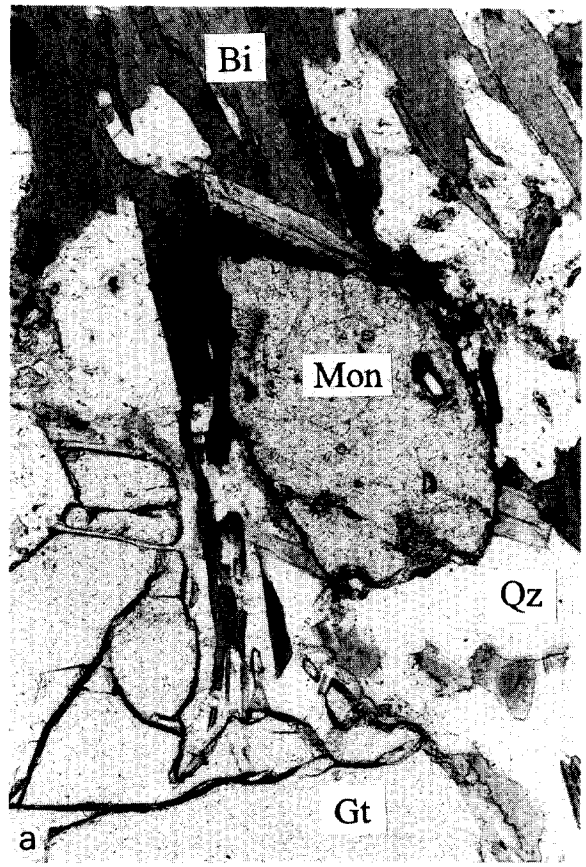

Fig. 1 (a). Transmitted light photograph of large monazite grain (Sample DW-9A) from felsic migmatite, Wind River Range, Wyoming. *Mon* = monazite; *Gt* = garnet; *Bi* = biotite; *Qz* = quartz.

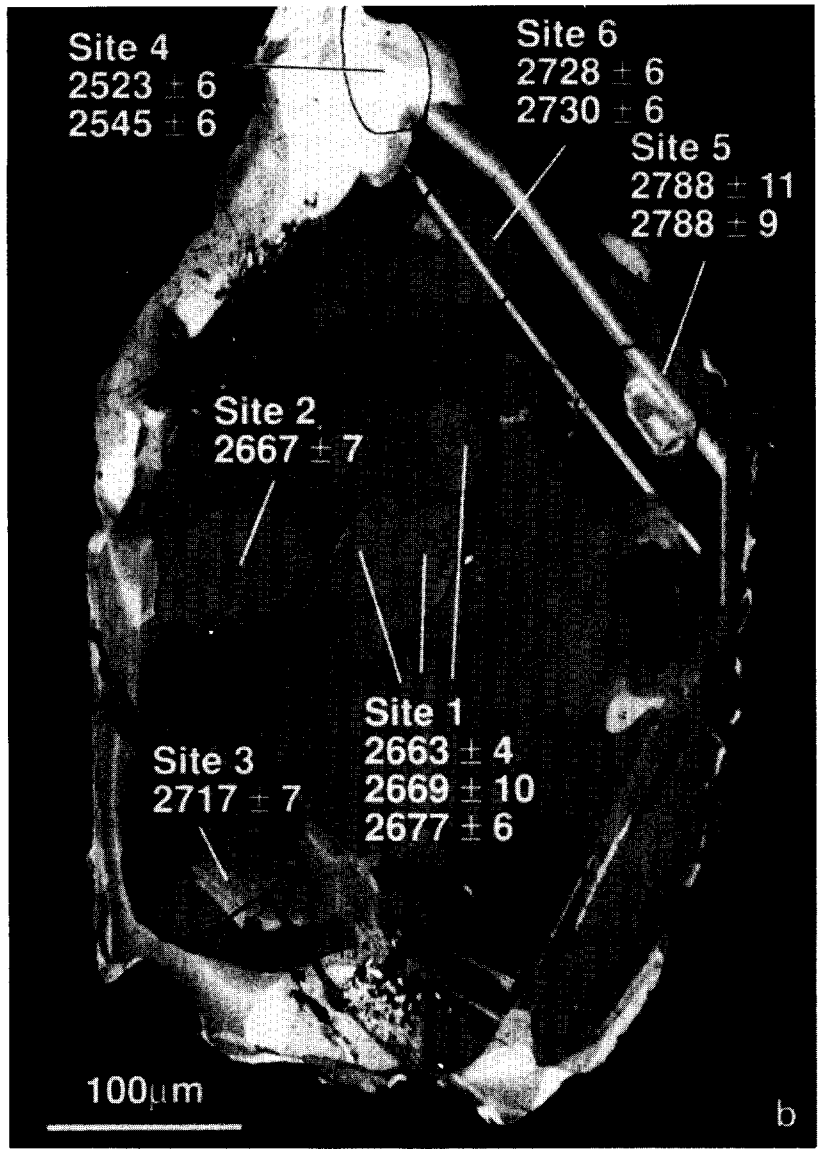

Fig. 1. (b). Back-scattered electron (BSE) photograph of the same grain. Six sites within the grain have been analysed by SIMS. Four of these sites are recognised on the basis of observed zonation: (5) Inclusion within lamellar zoned region, (6) lamellar zoned region, (1) partially re-homogenised (recrystallised?) core and (4) high contrast (high Th) apparently resorbed rim. Also in the grain are inclusions of quartz and biotite and an altered region with inclusions of $ThSiO_4$ (huttonite?) and apatite.

distinct zoned inclusion within the general region showing fine lamellar zoning; site 1, the core and bulk of the grain which shows a patchy zoning with isolated occurrences of high Th lamellar zones: and site 4, a resorbed (recrystallised?) high Th rim (Fig. 1b). These regions have distinctive major element compositions. The bulk of the grain contains a low amount (4–7%) of huttonite ($ThSiO_4$) component with 7–10% cheralite ($Ca_{0.5}Th_{0.5}PO_4$) component. In contrast, the region with the lamellar zoning exhibits a great range (3–15%) in huttonite component and lower

Table 1
TIMS data for groundmass monazite grains SW-121 [19]

SIZE	$\frac{^{206}Pb}{^{204}Pb}$	$\frac{^{207}Pb^*}{^{206}Pb}$	$\frac{^{208}Pb}{^{206}Pb}$	$\frac{^{207}Pb}{^{235}U}$	$\frac{^{206}Pb}{^{238}U}$	^{207}Pb age $\frac{}{^{235}U}$	^{206}Pb age $\frac{}{^{238}U}$	^{207}Pb age $\frac{}{^{206}Pb}$
150-180 μm	64840	0.1803 ± 0.0001	2.867 ± 0.003	12.73 ± 0.05	0.5118 ± 0.0021	2660 ± 4	2664 ± 8	2656 ± 2
120-150 μm	37084	0.1806 ± 0.0001	5.524 ± 0.006	12.72 ± 0.05	0.5109 ± 0.0022	2659 ± 5	2660 ± 9	2658 ± 2

cheralite contents (3–7%). The inclusion in the lamellar region (site 5) exhibits the same chemical variation as the lamellae which surround it and is considered to have grown at the same time. The high Th rim (site 4) contains up to 20% of both cheralite and huttonite components [21]. The fine scale lamellar zoning parallel to growth faces, and the irregular high Th rims are typical features of other monazites in this sample.

3. Analytical techniques

The isotopic compositions of Pb in individual monazites were obtained *in situ* from polished thin sections using the Cambridge ISOLAB-120. The performance of the ISOLAB-120 for SIMS Pb^+ analysis at high-resolving power has been detailed by Belshaw et al. [22]. In order to avoid major molecular interferences, ISOLAB is operated at 6000–7000 mass resolving power, similar to the operating conditions required for the analysis of Pb in zircons, ferromanganese samples and standard glasses [22]. A primary O^- beam focused to 20–50 μm, depending on analytical requirements produced a secondary Pb^+ beam from these monazites of ~3 cps/ppm Pb/nA O^-. This is relatively modest compared to the 20 cps/ppm Pb/nA O^- obtained from ferromanganese oxide samples [22] and highlights the large variation that exists in Pb^+ secondary ion yields from insulators for similar operating conditions.

Mass discrimination of Pb-isotopes using ISOLAB-120 in the SIMS mode has been assessed through the repeated analysis of NBS-610 glass and characterised natural ferromanganese samples and discrimination has been shown to be $< 0.2\%$ amu^{-1} [22]. Therefore, no corrections are made to the Pb-isotope ratio obtained here on monazites, and the accuracy of Pb-isotope ratio measurement is referenced to standard data reported from the Cambridge ISOLAB [22].

Masses ^{206}Pb, ^{207}Pb, and ^{208}Pb are resolved from molecular peaks at 6500 resolving power, such that potential interferences are estimated to be less than 0.002% at these masses, which is much less than the analytical uncertainty obtained during a typical analysis (0.25–0.5%). $^{206}Pb/^{204}Pb$ ratios have been measured and are in the range 3500 to 25,000. These are reproducible at a particular site, and do not correlate with $^{207}Pb/^{206}Pb$ ratios. They are lower overall than $^{206}Pb/^{204}Pb$ ratios of 37,000–65,000 measured by TIMS (Table 1), which might suggest some surface Pb-contamination or a very small unresolved molecular contribution at ^{204}Pb. The constancy of the $^{206}Pb/^{204}Pb$ ratio with time at each site argues against surface contamination and so far no interfering molecular has been identified. Even if all ions collected at mass 204 are assumed to be ^{204}Pb, correction of the $^{207}Pb/^{206}Pb$ ratio for common Pb ranges from about 0.5 to 2% of the ratio, which compares with typical 0.5% measurement precision.

As described in [22], the measurement precision exceeds counting statistics by a factor of 1.5–2. In contrast, the precision of $^{208}Pb/^{206}Pb$ ratios is poorer (1–2%) and frequently showed variation during the course of a run. For example, during one (extended) analysis, $^{208}Pb/^{206}Pb$ increased by 40% at constant $^{207}Pb/^{206}Pb$ (Fig. 3), demonstrating the existence of very fine scale (≤ 30 μm beam diameter) zoning in $^{232}Th/^{238}U$ ratio. The possible variability of the $^{207}Pb/^{206}Pb$ ratio in single grains of monazite has been assessed by the repeated analysis of three monazite

grains drawn from a monazite concentrate (120–180 μm) made from sample SW-121. Two aliquots from this concentrate, consisting of 3 and 7 grains respectively, have been analysed previously [19] by TIMS (Table 1). Both aliquots yielded concordant U–Pb ages with $^{207}Pb/^{206}Pb$ ages of 2656 ± 2 and 2658 ± 2 Ma, respectively. The SIMS results of spot analyses taken over these three grains are shown in Table 2 and Fig. 4. Grains 1, 2 and 3 yield average ages for all spots analysed of 2657 ± 25 Ma ($n = 8$), 2654 ± 59 ($n = 10$) and 2630 ± 8 ($n = 5$). Although the averages for grains 1 and 2 are close to the TIMS results the range of $^{207}Pb/^{206}Pb$ ages exceeds analytical precision. Some of these grains are markedly zoned and contain significant amounts of both cheralite and huttonite components [19]. In contrast, grain 3 is concentrically zoned with the chemical variation in the cheralite component only [19].

The abundances of Th, U and Pb in the monazites are sufficiently high to be measured by EPMA (Fig. 3). At this stage U/Pb and Th/Pb ratios have not been measured by SIMS due to the lack of suitable standards and accurate cali-

Table 2
SIMS data for groundmass monazite grains (Sample SW-121)

GRAIN	DATE-NUMBER	$^{207}Pb/^{206}Pb$	$^{208}Pb/^{206}Pb$	$^{206}Pb/^{204}Pb$	$^{207}Pb/^{206}Pb$ age
1	9-24-07	0.1809 ± 0.0006	5.19 ± 0.10		2661 ± 6
1	9-24-08	0.1812 ± 0.0010	6.57 ± 0.07		2663 ± 9
1	9-28-02	0.1806 ± 0.0016	7.61 ± 0.10		2658 ± 15
1	9-28-03	0.1799 ± 0.0013	6.87 ± 0.08		2652 ± 12
1	9-29-08,11	0.1824 ± 0.0007	7.02 ± 0.10	9900 ± 300	2674 ± 6
1	10-1-02	0.1806 ± 0.0023	8.69 ± 0.09		2658 ± 21
1	10-1-03	0.1807 ± 0.0012	8.81 ± 0.05		2659 ± 11
1	10-2-13,9	0.1774 ± 0.0009	5.92 ± 0.06	4700 ± 200	2628 ± 9
	MEAN	0.1805 ± 0.0028			2657 ± 25
2	9-24-04	0.1761 ± 0.0011	4.34 ± 0.04		2616 ± 10
2	9-24-05	0.1770 ± 0.0012	3.86 ± 0.03		2625 ± 11
2	9-24-07	0.1795 ± 0.0016	3.67 ± 0.03		2648 ± 15
2	9-24-09	0.1791 ± 0.0008	3.60 ± 0.01		2644 ± 7
2	10-1-05	0.1796 ± 0.0008	3.79 ± 0.02		2649 ± 7
2	10-1-06	0.1768 ± 0.0010	7.35 ±0.13		2623 ± 10
2	10-1-07	0.1853 ± 0.0007	3.98 ± 0.03		2701 ± 6
2	10-2-02,7	0.1808 ± 0.0013	3.26 ± 0.04	12,400 ± 900	2660 ± 12
2	10-2-03,6	0.1834 ± 0.0009	13.35 ± 0.06	15,200 + 1000	2684 ± 8
2	10-2-04,8	0.1846 ± 0.0011	3.67 ± 0.05	19,800 ± 2000	2694 ± 10
	MEAN	0.1802 ± 0.0065			2654 ± 59
3	9-29-03	0.1775 ± 0.0011	4.44 ± 0.03		2629 ± 10
3	9-29-04	0.1780 ± 0.0006	5.25 ± 0.04		2634 ± 6
3	9-29-05	0.1777 ± 0.0011	5.70 ± 0.05		2631 ± 10
3	9-29-06	0.1779 ± 0.0011	6.04 ± 0.03		2633 ± 10
3	10-3-03	0.1771 ± 0.0008	2.15 ± 0.04	24800 ± 1000	2625 ± 8
	MEAN	0.1776 ± 0.0009			2630 ± 8

Errors quoted for isotope ratios are $2\sigma_m$. Uncertainties quoted for $^{207}Pb/^{206}Pb$ ages correspond to the precision of isotope ratio measurement only.

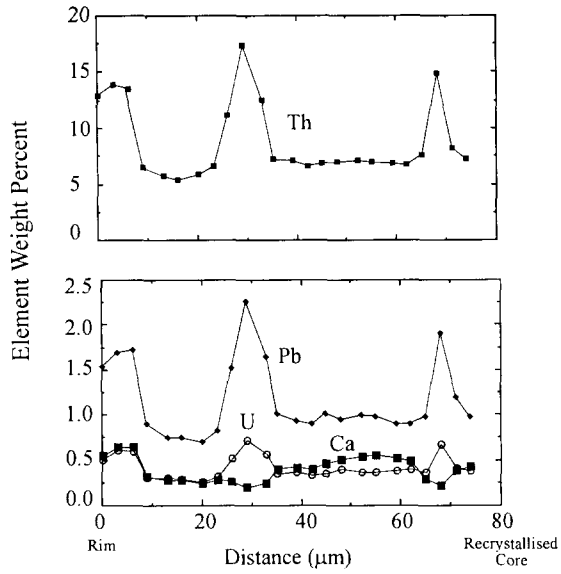

Fig. 2. Electron microprobe traverse across lamellar zoned region (site 6) of large grain (DW-9A). Large variations in Th, U and Pb concentrations are observed on a 1–3 μm scale. Note that there are no relative shifts in the concentration profiles of Th and Pb.

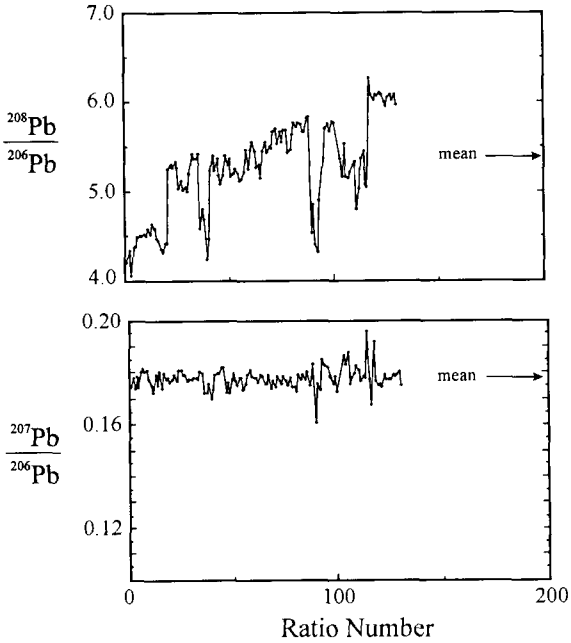

Fig. 3. The variation of $^{208}Pb/^{206}Pb$ and $^{207}Pb/^{206}Pb$ during the course of a run. The large increase in $^{208}Pb/^{206}Pb$ with time is attributed to small ($\ll 30$ μm) scale zonation in Th/U.

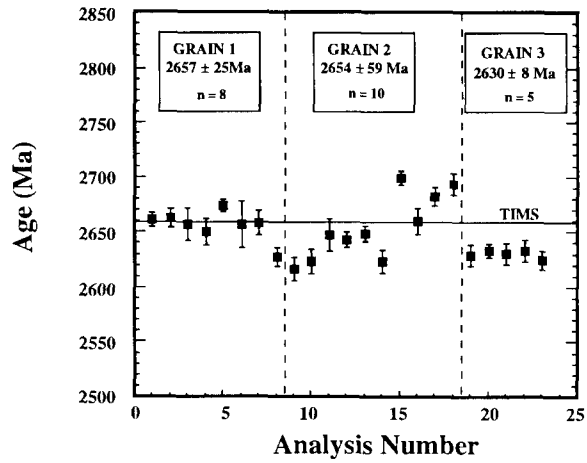

Fig. 4. Comparison of TIMS and SIMS ages for matrix monazite grains from SW 121. The scatter in grains 1 and 2 may result from real age structure in the grains. Single grains with homogeneous $^{207}Pb/^{206}Pb$ distribution at the micron scale may not exist in these samples.

bration techniques. A future aim must be to obtain Th/U and U/Pb ratios by both SIMS and EPMA on the same grains.

4. Results

4.1. Inclusions in garnet

Four monazite inclusions in the range of 10–50 μm diameter were analysed from a single garnet in sample DW-46 (Table 3; Fig. 5). Two of these monazites (DW-46.1,2), located in a portion of the garnet which is free from visible fractures, yield $^{207}Pb/^{206}Pb$ ages of 2781 ± 6 Ma and 2809 ± 10 Ma, that are apparently older than the matrix grains. Grain DW-46.4 is isolated in a feature, which appears as a hole, and which may be a fracture within the garnet. It yields an age (2669 ± 5 Ma) which is similar to TIMS ages on matrix monazites. DW-46.3, lies adjacent to, but not within, a large fracture and yields an intermediate age of 2764 ± 12 Ma. All of these grains have low Th contents (< 4%) and lower $^{208}Pb/^{206}Pb$ than the groundmass grains analysed.

Two additional monazite inclusions, both related to fractures within the garnet, have been

analysed in a garnet from SW-121. One of these, grain SW-121.2, is ca. 100 μm in diameter and occurs near the rim of a euhedral garnet, from which several fractures radiate and extend to the edge of the garnet. Four analyses of SW-121.3 yield $^{207}Pb/^{206}Pb$ ages that are within analytical uncertainty and give a mean age of 2606 ± 10 Ma (Table 3). The high $^{208}Pb/^{206}Pb$ ratios, between 8.89 and 9.42, correspond to a Th/U ratio of 30 and 32 for this age, which is typical of other high Th monazites from this sample [20]. Grain SW-121.1 is a ca. 50 μm inclusion located in a second euhedral garnet but in a fracture which extends to the edge of the garnet. A single analysis of this grain yields a $^{207}Pb/^{206}Pb$ age of 2623 ± 10 Ma (Table 3). Overall these results suggest that there may be substantial differences in the age preserved by monazite inclusions in garnets, depending upon whether or not they are located in fractures.

4.2. Single large groundmass grain

An attempt has been made to obtain Pb-isotope measurements from each of the three regions in the large grain from DW-9A shown in Fig. 1. Six sites were analysed and the results of these analyses are shown in Table 4. In Fig. 1, outlines of the regions analysed by SIMS have been superimposed on the BSE image, and represent the maximum area over which secondary Pb ions were collected. The oldest age obtained is from two analyses (site 5) in the rim where lamellar zoning is clearly preserved. The $^{207}Pb/^{206}Pb$

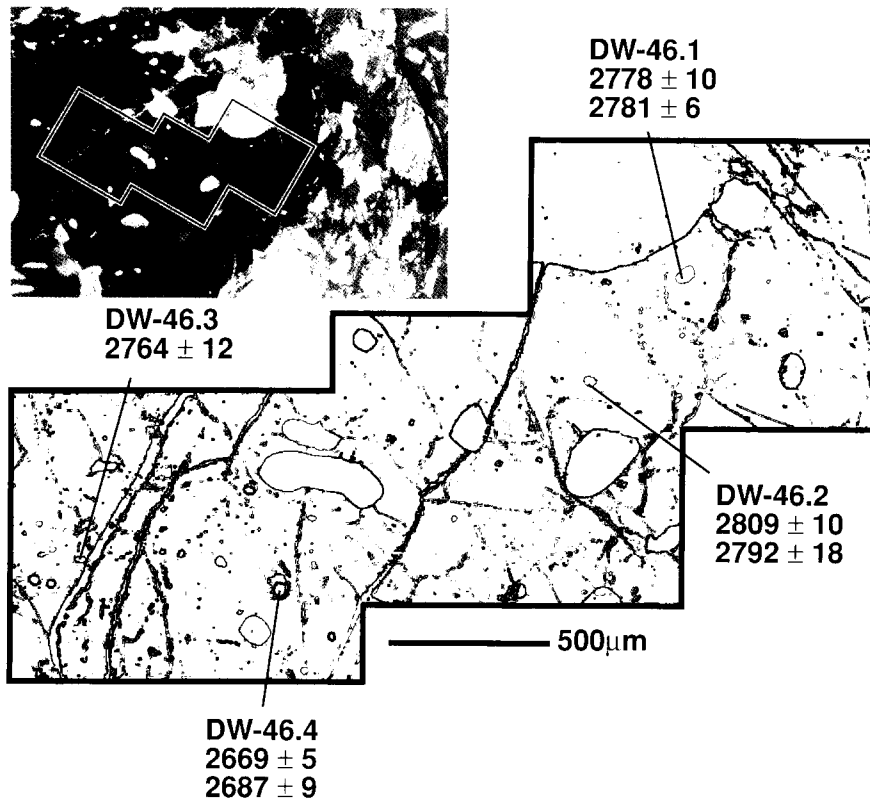

Fig. 5. Large garnet in DW-46 showing locations of monazites analysed by SIMS in relation to fractures and other inclusions which are mostly quartz.

Table 3
SIMS data for monazite inclusions in garnets

GRAIN DATE-NUMBER	$^{207}Pb/^{206}Pb$	$^{208}Pb/^{206}Pb$	$^{206}Pb/^{204}Pb$	$^{207}Pb/^{206}Pb$ age
SW-121.1 along fracture				
10-05-5,7	0.1768 ± 0.0011	0.774 ± 0.005	17500 ± 600	2623 ± 10
SW-121.3 along fracture				
9-30-02	0.1761 ± 0.0010	9.25 ± 0.04		2616 ± 9
9-30-03	0.1747 ± 0.0006	9.42 ± 0.05		2603 ± 6
10-01-04	0.1739 ± 0.0009	9.13 ± 0.06		2595 ± 9
10-05-01,3	0.1756 ± 0.0012	8.89 ± 0.09	9800 ± 700	2611 ± 11
DW-46.1 isolated				
10-08-02	0.1943 ± 0.0012	2.396 ± 0.004		2779 ± 10
10-08-03,5	0.1946 ± 0.0007	2.618 ± 0.010	22800 ± 2200	2781 ± 6
DW-46.2 isolated				
10-08-07,9	0.1980 ± 0.0012	1.465 ± 0.009	6600 ± 200	2809 ± 10
10-08-22	0.1959 ± 0.0021	1.525 ± 0.009		2792 ± 18
DW-46.3 adjacent to fracture				
10-08-12,14	0.1926 ± 0.0014	1.097 ± 0.004	6700 ± 400	2764 ± 12
DW-46.4				
10-08-17	0.1838 ± 0.0010	1.182 ± 0.003		2687 ± 9
10-08-18,20	0.1818 ± 0.0005	1.127 ± 0.006	15900 ± 1000	2669 ± 5

Errors as for Table 2.

ages obtained, 2788 ± 9 and 2788 ± 11 Ma respectively, are in good agreement. Site 6 straddles the apparent boundary between the lamellar and recrystallised zones and gives a slightly younger age. Four analyses (sites 1 and 2) in the recrystallised core yield ages of ca. 2665 Ma. A fifth analysis (site 3) in this region appears to have sampled both zoned and unzoned material, and yields an age of 2717 ± 9 Ma. Two analyses of the recrystallised or resorbed rim region give significantly younger ages of 2523 ± 6 and 2545 ± 6 Ma. The discrepancy between these two ages may result from incorporation of part of the lamellar zone in one analysis. This monazite grain in DW-9A apparently preserves a complex record spanning some 200 Ma! The oldest, zoned, portion of the grain agrees closely with the age obtained from the inclusions in the garnet phase that are remote from fracture and cracks.

5. Discussion

5.1. Assumptions in age interpretation

The significance of $^{207}Pb/^{206}Pb$ ages calculated from SIMS Pb-isotope analyses depends upon a number of factors. These are the possible uncertainties that might arise from common Pb, ^{206}Pb due to incorporation of excess initial ^{230}Th, inheritance of radiogenic Pb and the degree of U–Pb concordance of the monazite. Because $^{206}Pb/^{204}Pb$ ratios range from 3500 to 24,500 for the SIMS analyses reported here, the contribution (assuming that the entire contribution at 204 amu is from ^{204}Pb) is in most cases negligible. This point is evaluated further in Fig. 6, where the correction to the measured $^{206}Pb/^{204}Pb$ ratio is plotted as a function of measured $^{206}Pb/^{204}Pb$ ratio. For most analyses the correction does not

significantly exceed the analytical error; therefore, no correction for common Pb is made, and its contribution is not considered to significantly compromise the reported results. Several workers have stressed the effect of excess initial ^{230}Th on ^{206}Pb–^{238}U ages [13,15,23]. For SW-121 monazites analysed by TIMS (Table 1), the ^{206}Pb–^{238}U age is < 4 Ma greater than the ^{207}Pb–^{235}U age [19]. It is therefore assumed that the ^{207}Pb/^{206}Pb ages reported here are unlikely to be in error by more than (SIMS) analytical precision as a result of this effect. As monazites usually show a high degree of concordance in the U–Pb system it is assumed that calculated ^{207}Pb/^{206}Pb ratios provide good estimates of age, although in the absence of precise U/Pb ratio measurements this cannot be considered to be unequivocal.

5.2. *Age structures of monazite grains*

In the single large monazite grain (Sample DW-9; Fig. 1b) a clear relation exists between ^{207}Pb/^{206}Pb and details of the grain morphology and structure. The rim of the grain shows a lamellar zoning with zones of Th-enrichment (1–3 μm wide), and corresponding variations in Pb (Fig. 2). It also preserves the oldest age in the grain, close to the age obtained for the inclusions in the garnet (Table 2), and the age of presumed metamorphic zircons (ca. 2810 Ma) in SW-121 [19]. The zoned rim of the monazite is likely to record an age closest to the thermal maximum seen by this sample. Even at the high temperatures estimated for peak metamorphism (800°C) survival of chemical gradients attest to the very limited diffusive homogenisation of Pb that has occurred in this region of the grain.

The ^{207}Pb/^{206}Pb ages of the core of the grain appear to have been reset. Given the presence of a high Th overgrowth, with a ^{207}Pb/^{206}Pb age of 2535 ± 10 Ma, and the appearance of only partial homogenisation in the major elements (Fig. 1), interpretation of the intermediate apparent age

Table 4
SIMS data for zoned monazite (DW-9A)

GRAIN DATE-NUMBER	^{207}Pb/^{206}Pb	^{208}Pb/^{206}Pb	^{206}Pb/^{204}Pb	^{207}Pb/^{206}Pb age
site 1: core				
10-05-9,11	0.1812 ± 0.0004	4.942 ± 0.013	9900 ± 400	2663 ± 4
10-06-02,4	0.1827 ± 0.0007	4.409 ± 0.010	14800 ± 500	2677 ± 6
10-07-06,8	0.1818 ± 0.0011	4.440 ± 0.024	14300 ± 700	2669 ± 10
site 2: rim				
10-06-06	0.1816 ± 0.0008	5.364 ± 0.017		2667 ± 7
site 3: rim				
10-06-07,8	0.1871 ± 0.0008	5.916 ± 0.021	8500 ± 500	2717 ± 7
site 4: high Th rim				
10-07-02,4	0.1666 ± 0.0006	5.774 ± 0.029	9000 ± 300	2523 ± 6
10-07-10	0.1688 + 0.0006	5.750 ± 0.032		2545 ± 6
site 5: lamellar zone, inclusion				
10-07-12,14	0.1954 ± 0.0013	7.289 ± 0.032	3500 ± 100	2788 ± 11
10-09-02,5	0.1954 ± 0.0011	7.005 ± 0.028	4600 ± 100	2788 ± 9
site 6: adjacent to lamellar zone				
10-09-07	0.1884 ± 0.0007	5.101 ± 0.017		2728 ± 6
10-09-08,10	0.1886 ± 0.0006	4.822 ± 0.024	4200 ± 100	2730 ± 6

Errors as for Table 3.

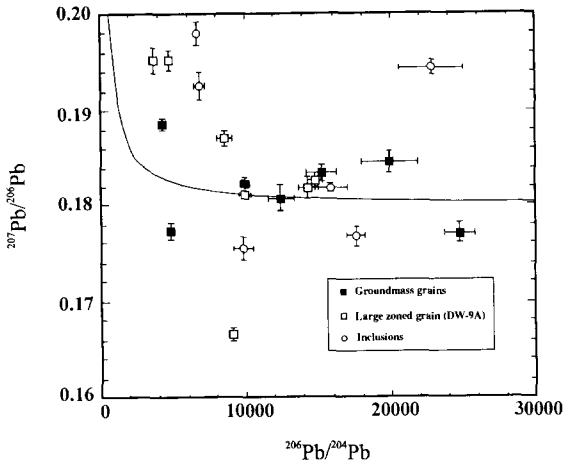

Fig. 6. $^{207}Pb/^{206}Pb$ versus $^{206}Pb/^{204}Pb$ for all data where both ratios were measured. No correlation is observed, as would be expected if common Pb were present. The curved line shows the influence of common lead with $^{207}Pb/^{206}Pb \sim 1.0$, on a sample with true $^{207}Pb/^{206}Pb = 0.18$, as a function of $^{206}Pb/^{204}Pb$ ratios. The lowest measured $^{206}Pb/^{204}Pb$ (3500) results in a $^{207}Pb/^{206}Pb$ correction of approximately 2%, which is larger than the typical analytical uncertainty (0.5%). However, typical $^{206}Pb/^{204}Pb$ result in corrections less than analytical error.

recorded in the core of the grain is not straightforward. Either the core was completely reset at ca. 2666 ± 8 Ma, or it was partially reset later, possibly at the time (2535 ± 10 Ma) of the high Th overgrowth. Several lines of evidence support complete re-equilibration at ca. 2665 Ma. First, this age is reproduced at two different sites in the core, with different $^{208}Pb/^{206}Pb$ ratios (4.4–5.4) corresponding to different Th/U ratios. Second, this age is in remarkably good agreement with the age determined for groundmass monazites by TIMS and SIMS from SW-121. Finally, this age is also close to the zircon age (2670 ± 13 Ma) determined on the syntectonic Bridger Batholith [11], the major lithologic component of the central and northern Wind River Range [24].

Preservation of older ages and primary lamellar zoning along the rim of the monazite grain indicates that the mechanism of resetting in the core is unlikely to be one of simple volume diffusion. If resetting occurred through recrystallisation, it must have occurred on a sub-grain scale, while preserving approximately the original crystallographic orientation, because there is no apparent change in extinction position across the grain. Black et al. [25] arrived at similar conclusions concerning the nature of recrystallisation of monazites from the Napier Complex using TEM. These authors noted that the monazite grains were composed entirely of ca. 100 Å crystalline domains, which although non-metamict arose from radiation damage. Because the age of the core of the monazite grain studied here is only ~ 100 Ma younger than the undisturbed portion of the grain, the amount of radiation damage over this interval would have been small. It seems unlikely that resetting of the age in this case results from radiation damage.

5.3. Relation of inclusions to garnet growth and closure

The SIMS analyses of monazite inclusions in garnet (Table 3) preserve the oldest ages where they are remote from fractures. In these cases the ages are similar to the age found for the remnant zoned rim of the large single monazite grain (Fig. 1b). On the other hand, where the inclusions are located within or adjacent to the fractures their ages are similar to the 'recrystallised' core of the large monazite grain. Several observations lead to the conclusion that the monazites in the garnets in SW-121 are metamorphic and likely grew at the same time as the garnets. First, there is a clear association of monazites with garnet in these samples [21]; 75% of all monazite grains occur in garnet although garnet comprises less than 15% of the rock. Second, the monazite inclusions show no textural or chemical evidence for resorption or overgrowths as would be expected if they were detrital and had been exposed to low grade metamorphic conditions where monazite may be unstable. Instead, they are typical in size (< 50 μm), morphology (round to tabular with aspect ratio less than 2), and chemistry to monazites from other upper amphibolite grade terranes [13,15,21,27]. Third, the age range of the monazite inclusions overlaps the concordia U–Pb age of two zircons analysed by TIMS [19] which have a rounded, football-shaped, morphology indicative of metamorphic origin.

These SIMS measurements on monazite inclusions also shed some light on the TIMS U–Pb measurements on garnets. Fission track distributions and stepwise dissolution experiments on garnets in SW-121 demonstrate that monazite dominates the U budget of the garnet and controls the U–Pb age obtained on bulk garnets [19]. These results suggest that it is access of some of these monazite inclusions to fractures in the garnet, and their consequent resetting, that results in the variation in U–Pb ages between different aliquots of SW-121 garnets analysed by TIMS [19]. All of the TIMS U–Pb garnet ages and nearly all of the SIMS $^{207}Pb/^{206}Pb$ ages on monazite inclusions are older than the TIMS Sm–Nd garnet-matrix isochron age of 2598 ± 12 Ma [19]. Garnet U–Pb ages are consistently older than matrix monazite age and garnet-matrix Sm–Nd age in upper amphibolite and granulite facies rocks [5,16,28]. In order to ascribe this observation to lower diffusivity of Pb relative to Nd, the relationship needs to be demonstrated on garnets where the monazite contribution to the Pb-budget is demonstrably small.

The preservation of old $^{207}Pb/^{206}Pb$ ages in monazite inclusions most probably arises from the armouring property of large garnet porphyroblasts. With negligible Pb to exchange, garnet armours the monazite, enabling the U–Pb system in the inclusions to remain closed. To the extent that the U budgets of almandine-pyrope garnets are dominated by monazite inclusions, this process may be a general one.

The SIMS results also yield insight into the timing and cause of fracturing in the SW-121 garnets. Garnets often display fractures that radiate away from inclusions, especially where they are rich in U and Th. In the SW-121 garnets, the fractures presumably developed at about the same time as the monazite inclusions located within them were isotopically reset, i.e., 2605–2675 Ma. If experimental [26] and empirical [16,28] estimates of the closure temperature for the Sm–Nd system in garnet (ca. 600–650°C) are correct, these garnets must have been cooled through this temperature range at 2598 ± 12 Ma, the Sm–Nd age determined for these garnets [19], suggesting that the fractures were active at temperatures about 650°C. This is consistent with the observation that garnets from SW-121 and other samples in the Crescent Lake area have elevated Fe contents along some fractures, indicative of retrograde Fe–Mg exchange with biotite. The case against volume diffusion being the operative process determining the age distribution in monazite is strengthened by the lack of correlation between grain size and time of resetting. The largest inclusion grain (ca. 100 μm; SW-121.3), which is closest in size to the groundmass grains analyse by TIMS (150–180 μm), records the youngest age.

5.4. A metamorphic chronology from monazites

The existence of several episodes of large scale magmatism in the Wind River Range during the Archean has been established [20]. The syntectonic Bridger Batholith yields zircon ages of 2.67 Ga [11] and the Louis Lake and post-tectonic Bear Ears plutons yield ages of 2.63 and 2.55 Ga, respectively [20]. However, the temporal relationship between magmatism and regional metamorphism of the country rock is unclear. If zircons and monazite inclusions in garnets (2.77–2.82 Ga) from sample SW-121 record prograde metamorphism, regional metamorphism must have preceded the emplacement of the Bridger Batholith by at least 100 Ma. The only other evidence for metamorphism at this time is from the central Wind Rivers, ca. 2.85 Ga zircon cores from a charnockite analysed by SIMS [11]. If the original growth occurred at 2.77–2.82 Ga, this time may be correlated with the peak conditions (800 ± 50°C; 8 ± 1 kb) determined by Sharp and Essene [1] using mineral inclusions in pelitic garnets.

Groundmass monazite U–Pb ages record a later event which accompanied at least temporarily the emplacement of the Bridger Batholith at 2.67 Ga. Based on the mottled textures and lack of distinct lamellar zoning in the SW-121 monazites, and the clear evidence for recrystallisation in the DW-9A monazites, this was most likely a time of resetting of pre-existing monazite rather than growth of new monazite, although the latter possibility cannot be ruled out. The Sm–Nd ages on garnets record cooling through a closure temperature of 600–650°C at 2598 ± 12 Ma. An al-

lanite age from an essentially undeformed pegmatite of 2607 ± 4 Ma indicates that deformation ceased by this time, but that anatectic conditions continued on a very localised scale [24].

6. Concluding remarks

The utility of SIMS techniques for the study of Archean monazite $^{207}Pb/^{206}Pb$ chronology is demonstrated by this study. The technique of *in situ* analysis has the great advantage of being able to relate the metamorphic phases which provide age information to details of metamorphic textures and minerals.

Furthermore, *in situ* measurement of Pb isotope ratios in monazite by SIMS should be a useful tool in addressing questions related to the pathways of fluid flow in metamorphic rocks and the mechanisms of resetting of U–Pb isotope systematics in minerals. The results obtained here strongly suggest that monazite may be reset, not by volume diffusion, but by fluid-mediated recrystallisation. If further studies indicate this to be a general phenomenon, it will add to the requirement for a reassessment of models of isotope closure of minerals that are simply based on volume diffusion. Analytical precisions obtained correspond to age uncertainties of 4–5 Ma for samples of Archean age. This precision obtained with SIMS is within the thermal time constants associated with regional metamorphism and may eventually allow the determination of growth rates of major phases which have occluded monazite inclusions during their development. Thorough studies of the major element chemistry coupled with SIMS study of monazite may afford access to a substantial part of the metamorphic history of many ancient regional terranes.

Acknowledgements

This research has been supported in Cambridge by NERC and the Royal Society. The authors are grateful for the support provided to CPD by the Scott Turner Fund of the University of Michigan and NSF grants 82-12764, 90-04302 and 91-17772, to Prof. E.J. Essene. Thanks to A.N. Halliday and E.J. Essene for discussion and review, and to Zach Sharp for providing thin sections and initial advice in field work. Dale Austin (UM) drafted some of the figures, and Dave Martel helped in preparation of the final manuscript and some figures.

References

[1] Z.D. Sharp and E.J. Essene, Metamorphic conditions of and Archean core complex in the northern Wind River range, Wyoming, J. Petrol. 32, 241–273, 1991.

[2] D. Vance and R.K. O'Nions, Isotope chronometry of zoned garnets: growth kinetics and metamorphic histories. Earth Planet. Sci. Lett. 97, 227–240, 1990.

[3] K.W. Burton and R.K. O'Nions, High resolution garnet chronometry and rates of tectonometamorphic processes, Earth Planet. Sci. Lett. 107, 649–671, 1991.

[4] J.N. Christensen, J.F. Rosenfeld and D.J. DePaolo, Rates of tectonometamorphic processes from rubidium and strontium isotopes in garnet, Science 244, 1465–1469, 1989.

[5] K.W. Burton and R.K. O'Nions, The timing of mineral growth across a regional metamorphic sequence, Nature 357, 235–238, 1992.

[6] K. Mezger, G.N. Hansen and S.R. Bohlen, U–Pb systematics of garnet in the late Archean Pikwitonei granulite domain at Cauchon and Natawahunan lakes, Manitoba, Canada, Contrib. Mineral. Petrol. 101, 136–148, 1989.

[7] D.O. Froude, T.R. Ireland, P.D. Kinney, I.S. Williams, W. Compston, I.R. Williams and J.S. Myers, Ion microprobe identification of 4100–4200 Ma terrestrial zircons, Nature 304, 616–618, 1983.

[8] W. Compston, I.S. Williams and C. Meyer, U–Pb geochronology of zircons from Lunar Breccia 73217 using a sensitive high mass-resolution ion microprobe, Proc. XIV Lunar Planet Sci. Conf. J. Geophys Res 89 Suppl., B525, 1984.

[9] I.S. Williams, W. Compston, L.P. Black, T.R. Ireland and J.J. Foster, Unsupported radiogenic Pb in zircon: a cause of anomalously high Pb–Pb, U–Pb and Th–Pb ages, Contrib. Mineral. Petrol. 88, 322, 1984.

[10] W. Compston, P.D. Kinney, I.S. Williams and J.J. Foster, The age and Pb loss behaviour of zircons from the Isua supracrustal belt as determined by ion microprobe, Earth Planet. Sci. Lett. 80, 71–81, 1986.

[11] J.N. Aleinikoff, I.S. Williams, W. Compston, J.S. Stuckless, and R.G. Worl, Evidence for an Early Archean component in the Middle to Late Archean gneisses of the Wind River Range, west-central Wyoming: conventional and ion microprobe U–Pb data, Contrib. Mineral. Petrol. 101, 198–206, 1989.

[12] P.K. Zeitler, B. Barriero, C.P. Chamberlain and D. Rumble, Ion-microprobe dating of zircon from quartz-graphite veins at the Bristol, New Hampshire, metamorphic hot spot, Geology 18, 626–629, 1990.

[13] W.C. Overstreet, The geologic occurrence of monazite, US Geol. Surv. Prof. Pap. 530, 1967.

[14] R.R. Parrish, U–Pb dating of monazite and its application to geological problems, Can. J. Earth Sci. 17, 1431–1450, 1990.

[15] W.N. Sawka, J.F. Banfield and B.W. Chappell, A weathering-related origin of widespread monazite in S-type granites, Geochim. Cosmochim. Acta 50, 171–175, 1986.

[16] H.A. Smith and B.A. Barriero, Monazite U–Pb dating of staurolite grade metamorphism in pelitic schists, Contrib. Mineral. Petrol. 105, 602–615, 1990.

[17] K. Mezger, E.J. Essene and A.N. Halliday, Closure temperatures of the Sm–Nd system in metamorphic garnets, Earth Planet. Sci. Lett. 113, 397–409, 1992.

[18] D. Vance, N.S. Belshaw and R.K. O'Nions, U–Pb chronometry of metamorphic garnets: a comparison of TIMS analyses of garnet and high resolution SIMS analysis of U-rich inclusions, Eos 72, 560, 1991.

[19] C.P. DeWolf, A.N. Halliday, E.J. Essene, K. Mezger and C. Zeissler, Evaluating the role of inclusions in U–Pb and Sm–Nd garnet geochronology: stepwise dissolution experiments and induced fission track distributions, Eos 73, 652, 1992.

[20] J.S. Stuckless, C.E. Hedge, R.G. Worl, K.R. Simmons, I.T. Nkomo and D.B. Wenner, Isotopic studies of the late Archean plutonic rocks of the Wind River Range, Wyoming, Geol. Soc. Am. Bull. 96, 850–860, 1985.

[21] C.P. DeWolf and E.J. Essene, Chemical variations in monazite as records of metamorphic histories, *in prep.*

[22] N.S. Belshaw, R.K. O'Nions, D.J. Martel and K.W. Burton, High resolution SIMS analysis of common lead, Chem. Geol. (in press).

[23] U. Scharer, The effect of initial ^{230}Th disequilibrium on young U–Pb ages: the Makalu case, Himalaya, Earth Planet. Sci. Lett. 67, 191–204, 1984.

[24] C.P. DeWolf, Metamorphic geochronology of a high grade gneiss terrane, Ph.D. thesis, Univ. Michigan, 1993.

[25] R.G. Worl, M.E. Koesterer and T.P. Hulsebosch, Geologic map of the Bridger Wilderness and Green-Sweetwater roadless area, Sublette and Fremont counties, Wyoming. US Geol. Surv. Map MF-1636-B: scale 1:250,000, 1986.

[26] L.P. Black, J.D. Fitzgerald and S.L. Harley, Pb isotopic composition, colour and microstructure of monazites from a polymetamorphic rock in Antarctica, Contrib. Mineral. Petrol. 85, 141–148, 1984.

[27] R.A. Coughlan, Studies in diffusional transport: grain boundary transport of oxygen in feldspars, diffusion of oxygen and strontium and the REEs in garnet, and thermal histories of granitic intrusions in south-central Maine using oxygen isotopes, Ph.D. thesis, Brown University, 238 pp., 1990.

[28] H.A. Smith, C.P. Chamberlain and P.K. Zeitler, Documentation of Neogene regional metamorphism in the Himalayas of Pakistan using U–Pb in monazite, Earth Planet. Sci. Lett. 89, 239–259, 1992.

[29] K.W. Burton, A.S. Cohen and R.K. O'Nions, Sm, Nd, U and Pb diffusion in garnet, Terra Abstr. 5, 382, 1993.